

Probabilistic Speech-Driven 3D Facial Motion Synthesis: New Benchmarks, Methods, and Applications

Karren D. Yang, Anurag Ranjan, Jen-Hao Rick Chang, Raviteja Vemulapalli, Oncel Tuzel
Apple

{karren_yang, anuragr, jenhao.chang, r_vemulapalli, ctuzel}@apple.com

Abstract

We consider the task of animating 3D facial geometry from speech signal. Existing works are primarily deterministic, focusing on learning a one-to-one mapping from speech signal to 3D face meshes on small datasets with limited speakers. While these models can achieve high-quality lip articulation for speakers in the training set, they are unable to capture the full and diverse distribution of 3D facial motions that accompany speech in the real world. Importantly, the relationship between speech and facial motion is one-to-many, containing both inter-speaker and intra-speaker variations and necessitating a probabilistic approach. In this paper, we identify and address key challenges that have so far limited the development of probabilistic models: lack of datasets and metrics that are suitable for training and evaluating them, as well as the difficulty of designing a model that generates diverse results while remaining faithful to a strong conditioning signal as speech. We first propose large-scale benchmark datasets and metrics suitable for probabilistic modeling. Then, we demonstrate a probabilistic model that achieves both diversity and fidelity to speech, outperforming other methods across the proposed benchmarks. Finally, we showcase useful applications of probabilistic models trained on these large-scale datasets: we can generate diverse speech-driven 3D facial motion that matches unseen speaker styles extracted from reference clips; and our synthetic meshes can be used to improve the performance of downstream audio-visual models.

1. Introduction

Recently, there has been significant research interest in animating 3D faces from speech signals [9, 10, 16, 33, 38] with potential applications across immersive interactions, content creation and synthetic data generation. Most existing works approach this problem by learning a *deterministic* mapping from speech to 3D face meshes in a data-driven

manner [9, 10, 16, 38], leveraging advancements in deep learning. These methods are typically optimized on small datasets containing 10-20 speakers [9, 17] and can achieve high-quality lip reconstruction for the speakers in the training dataset [9, 16, 38]. However, these methods fall short of capturing the *one-to-many* relationship between speech and realistic facial motions.

Animating 3D faces from speech is a complex problem. For a given speech utterance, there exists a multi-modal distribution of plausible facial motions capturing large variations in speaking style across a population. Even for a single speaker, the conditional distribution of facial motions given speech is multi-modal, capturing intra-speaker variations such as emotions [10] and other paralinguistic cues that give nuance to the meaning of the speech. Modeling this complex, one-to-many relationship between speech and 3D facial motion necessitates a *probabilistic* approach, since approximating a multi-modal distribution with a deterministic point estimate leads to predicting the mean [9, 16] or a single mode [38] of the conditional distribution.

1.1. Challenges

Datasets. Learning this multi-modal distribution poses new challenges for the field of speech-driven 3D facial animation. First is the limitation of existing datasets. Building a useful probabilistic model that captures the wide variety of speech and facial motions requires a large amount of data from many speakers. However, existing public datasets are small and contain utterances from few speakers [9, 17], thus offering limited opportunity for learning diverse 3D facial motions. While a large-scale dataset is used in MeshTalk [33], this dataset is proprietary and not available to the research community.

Metrics. The second challenge is the lack of proper evaluation metrics for probabilistic speech-driven facial motion synthesis. Existing works use lip vertex error as the primary metric for evaluating lip synchronization [9, 33]. While lip vertex error is a useful proxy for lip articulation quality, it presumes a one-to-one relationship between speech and lip motion and penalizes realistic variations from the con-

ditional mean. Other metrics such as upper-face dynamics deviation (FDD) have been proposed to measure the variability of the upper face, but they still compare the generated 3D facial motion against an absolute ground truth [38]. There is a need for metrics that are more suitable for evaluating lip quality and diversity in a probabilistic setting.

Modeling. Third, while learning to model the full distribution paves the way for realistic facial motions, it also opens the door to generating samples that are unexpected or even of lower fidelity [32]. As humans are sensitive to facial cues and expressions, it is crucial for facial motions to be constantly in sync with speech, as any inconsistent motions would be glaringly obvious to a viewer. Most existing probabilistic models in other domains do not consider this problem, as their conditioning signals have weaker correlation with the synthesized content. Therefore, there is a need for modeling techniques that can achieve diverse facial motions while maintaining fidelity to the driving speech signal. Ensuring speech synchronization is made more difficult when also considering the need for other conditioning inputs, namely speaking style. Most existing works do not consider these challenges or interactions as they use one-hot speaker encodings and are not intended to generalize to unseen speaking styles.

1.2. Contributions

In this work, we address these challenges with new large-scale datasets, metrics, and modeling techniques for probabilistic speech-driven 3D facial animation.

Datasets. We propose a novel benchmark dataset for studying probabilistic speech-driven 3D facial motions based on two large-scale paired audio-mesh datasets derived from the VoxCeleb2 [7] video dataset using state-of-the-art monocular face reconstruction methods [18, 19]. Our proposed audio-mesh datasets contain thousands of speakers and are orders of magnitude larger than current public benchmarks [9, 17].

Metrics. We introduce metrics that are suitable for evaluating probabilistic models. We propose to quantify how well probabilistic models generate samples close to the ground truth lip motion, allowing a more comprehensive picture of lip articulation quality that takes the diversity of probabilistic models into account. We also train audio-mesh synchronization models and speaker recognition models to measure other aspects of generative quality, such as synchronization, realism, and diversity.

Modeling. We demonstrate a two-stage probabilistic autoregressive model over residual vector-quantized codes that achieves diverse generation while maintaining robust synchronization with speech. We show that a standard design of a two-stage probabilistic autoregressive model that is conditioned on both speech signal and a style reference weakens lip synchronization, and propose a design that can

match the speaking style of the reference without sacrificing synchronization quality. We also demonstrate simple but effective sampling strategies for trading off diversity for better lip precision and speech synchronization.

Results. We use our metrics to analyse prominent deterministic (VOCA [9], Faceformer [16], CodeTalker [38]) and non-deterministic methods (MeshTalk [33]) on the large-scale datasets. Our approach outperforms these existing methods, demonstrating the potential of probabilistic modeling. In perceptual studies, our approach is rated as producing more realistic lip and upper face motion, as well as more capable of capturing inter-speaker diversity (*i.e.*, matching reference clips) compared to deterministic models. Synthetic lip meshes generated from our method can be used to train downstream audio-visual models. On the challenging task of noisy audio-visual speech recognition on LRS3 [1], we improve relative WER by 11.3% compared to a model that is trained on the ground truth corpus and 47.0% compared to meshes from a deterministic model.

2. Related Work

Speech-driven face animation is a highly active field with extensive literature. Existing works can be grouped as follows. First, there are *viseme-based* methods that map the phonetic components of speech to their visual counterparts. Second, there are *video-based* methods that aim to produce convincing outputs in the pixel space. Third and most relevant to our work, there are *3D animation* methods that drive facial motion as represented by 3D facial landmarks or meshes using speech signals.

Note there is overlap between these groups, in that some of the photorealistic methods also produce intermediate 3D outputs such as facial landmarks or meshes. However, we draw the distinction depending on whether the techniques mainly focus on the 3D facial geometry or on the photorealistic video quality.

Viseme-Based Methods. Early methods use linguistic observations [4, 28, 35, 39] to map from phoneme to viseme sequences. Phonemes are derived directly from text [2, 14, 15] or from speech via acoustic models [37]. Viseme sequences are subsequently translated to animations by morphing templates [14, 15, 23, 24] or 3D rigged models as in JALI [13]. More recently, deep learning methods have been introduced to learn the mapping function from phonemes to visemes [34, 41]. While viseme-based methods provide interpretable controls over lip motion, their expressive power is limited; for example, they cannot produce subtle facial gestures in other regions of the face.

Video-Based Methods. There is extensive literature on synthesizing photorealistic talking heads from speech inputs. Most of these works synthesize 2D talking head videos [5, 6, 20, 29, 40] and cannot easily be extended

to 3D. Some recent methods incorporate neural rendering pipelines to synthesize 3D talking heads that can be rendered from different camera angles [21], but they usually require speaker- or scene-specific training. In general, these methods focus on minimizing errors over the pixels of a video, rather than explicitly modeling 3D facial motions.

3D Animation Methods. Several previous works propose speaker-specific models that need to be trained on personalized data and cannot be used in generic settings [25]. Early multi-speaker methods produce low-dimensional features such as blendshape coefficients [12]. Recent methods focus on animating the entire face from speech by directly operating in the vertex space [9, 10, 16, 33, 38]. However, these methods mostly consider a deterministic formulation of the task. VOCA [9] and Faceformer [16] formulate speech-driven animation as a direct regression problem. In CodeTalker [38], the authors explicitly point out this limitation of previous work; even so, their proposed approach does not model the full conditional distribution, but rather projects the output of a regression function to a mode learned from a discrete motion codebook.

Meshtalk [33] proposes a probabilistic method based on learning an auto-regressive model over discrete codes. To enforce a correlation between speech and facial motions, lower face vertices are regressed from the speech signal and upper face vertices are reconstructed from ground truth meshes through the bottleneck of a discrete Gumbel-Softmax auto-encoder [33]. Subsequently, a probabilistic auto-regressive model is trained over the codes conditioned on speech. While the regression strengthens the correspondence between the speech signal and the generated lip motion, it limits the quality and diversity of the lower face.

In the context of dyadic 3D facial motion synthesis, Ng *et al.* [30] propose a probabilistic auto-regressive model for generating a listener’s facial motions in a two-person conversation. However, the task differs from ours, in that while the listener’s expressions are correlated with the speaker’s voice and motions, this correlation is inherently weaker than in speech-driven facial motion.

3. Approach

Our goal is to learn a probabilistic model $p_G(\mathbf{x}|\mathbf{y}, \mathbf{s})$ to synthesize 3D facial motion from speech, where $\mathbf{x} \in \mathbb{R}^{T \times 3V}$ is the target sequence of 3D mesh deformations, $\mathbf{y} \in \mathbb{R}^{T \times D_y}$ is the driving speech signal, and $\mathbf{s} \in \mathbb{R}^{T_s \times 3V}$ is a reference speaker sequence of 3D mesh deformations for controlling inter-speaker variation. We propose to first discretize the space of 3D facial motion using a *residual* vector-quantized (RVQ) codebook in a coarse-to-fine manner (Figure 1a, Section 3.1). Then, we propose an effective architecture for learning a two-stage probabilistic auto-regressive model over the codes (Figure 1b, Section 3.2). Finally, we propose sampling strategies to trade-off diver-

sity for improved precision and speech synchronization, and propose a knowledge distillation strategy to amortize the sampling overhead (Section 3.3).

3.1. RVQ for 3D Facial Motion

Let \mathcal{C} denote a fixed-size codebook with codes of size N_C . Residual vector quantization [27] is a discretization technique that recursively projects a vector $\mathbf{z} \in \mathbb{R}^{N_C}$ to the nearest code in \mathcal{C} and takes the residual. After D steps, \mathbf{z} can be represented by an ordered sequence of indices for the codes in \mathcal{C} , and the quantization of \mathbf{z} up to depth d is represented by summing the codes corresponding to those indices. We apply RVQ to obtain a coarse-to-fine discretization of 3D facial motion by performing the above recursion within the latent space of a 3D facial motion autoencoder, as shown in Figure 1a. Specifically, we use a temporal convolutional encoder to map \mathbf{x} to a latent embedding of motion, $Z \in \mathbb{R}^{T \times N_C}$. Each temporal index of Z is separately quantized using RVQ, and the quantized latent embedding of motion is decoded back to the 3D motion space using a convolutional decoder. The encoder and decoder of this autoencoder are jointly optimized via gradient updates to minimize reconstruction loss through the discrete code using a straight-through estimator [36]. The use of a commitment loss [27] to penalize the error of the quantization at every depth effectively ensures that the meshes can be reconstructed from the codes in a coarse-to-fine manner.

3.2. Two-Stage Probabilistic AR Model

From RVQ autoencoder, we obtain the codebook indices of a 3D mesh sequence \mathbf{x} . We denote these by a matrix \mathbf{j} , where j_{td} denotes the index for time point t and depth d . Next, we predict the individual code indices of \mathbf{j} conditioned on \mathbf{y} and \mathbf{s} ,

$$\prod_{d=1}^D \prod_{t=1}^T p(j_{td} | \mathbf{j}_{<t}, \mathbf{j}_{t,<d}, \mathbf{y}_{\leq t}, \mathbf{s}), \quad (1)$$

using a two-stage [27] probabilistic Auto Regressive (AR) model consisting of a temporal model and a depth model (Figure 1b). The temporal model is an auto-regressive model that produces an audio-visual embedding for each time frame t capturing historical audio-visual context as well as the audio embedding from t :

$$\mathbf{h}_{av}[t] = \text{TemporalModel}(\mathbf{y}_{\leq t}, \tilde{e}(\mathbf{j}_{t-1}), \tilde{e}(\mathbf{j}_{t-2}), \dots) \quad (2)$$

where $\tilde{e}(\mathbf{j}_t) := \sum_d e(j_{td})$ and $e(i)$ indicates the code in \mathcal{C} corresponding to the i -th index. We experiment with both causal convolutional and transformer auto-regressive architectures for temporal model and find that the longer context of a transformer offers limited benefit when context information is provided through a reference style clip (see Supplemental Materials).

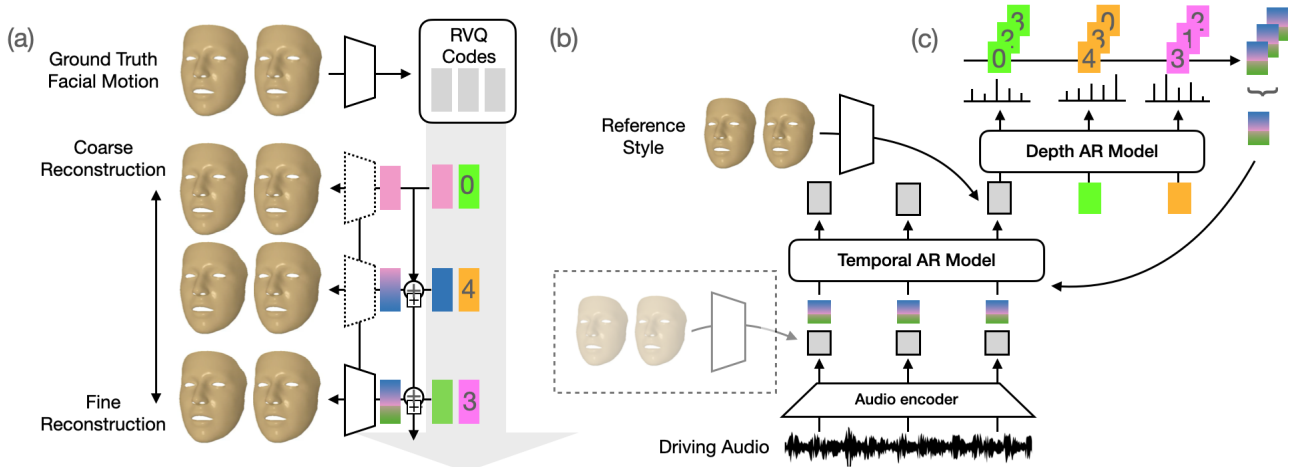


Figure 1. **Method Overview.** We learn a probabilistic model to synthesize 3D facial motion. (a) We first learn a residual vector-quantized codebook over the space of 3D facial motion. (b) We then train a two-stage, probabilistic auto-regressive model to predict these codes in a coarse to fine manner conditioned on audio and a reference speaker clip. (c) During inference, we propose simple and effective sampling strategies to trade-off the diversity of the model in favor of improved lip fidelity.

Subsequently, the depth model uses the audio-visual context captured in $\mathbf{h}_{av}[t]$ to generate each of the D code indices for the current time frame in an auto-regressive manner. The depth model consists of a masked self-attention transformer block which, at time frame t , operates along a length $D + 1$ sequence v_t defined as: $v_{t1} = p_1 + E_s(\mathbf{s})$, $v_{t2} = p_2 + \mathbf{h}_{av}[t]$, and $v_{td} = p_d + \sum_{d'=1}^{d-1} e(j_{td'})$ for $d \geq 3$, where p_i denotes a learned positional encoding. The output of the depth model is a prediction of the conditional distribution of the next token.

$$p(j_{td} | j_{t, < d}, \mathbf{h}_{av}[t], \mathbf{s}) = \text{DepthModel}(v_{t, \leq d+1}) \quad (3)$$

Notice that we incorporate the encoded \mathbf{s} as the first token input into the depth transformer, effectively shifting the standard input sequence by one. We find that incorporating speaker information as an input to the second-stage model, rather than as an input to in the first-stage model, which is more standard [27] and is showed as the grayed out box in Figure 1(b), is crucial for proper speech synchronization. As we show in Table 3, incorporating the speaker information into the first stage model rather than the second results in a decrease in synchronization. The two-stage auto-regressive model is trained end-to-end to minimize the cross-entropy loss, $-\mathbb{E}_{t,d} \log p(j_{td} | \mathbf{j}_{<t}, \mathbf{j}_{t, < d}, \mathbf{y}_{\leq t}, \mathbf{s})$, in a teacher-forcing manner.

3.3. Trading off Diversity

During inference, we can sample from the conditional distribution of facial motions as shown in Equation 1. This achieves good results but we also want to control the diversity/variability of the synthesis. In particular, the training

loss forces the probabilistic AR to capture the entire training distribution of codes, which is noisy and can result in sampling codes that are less faithful to the conditioning speech during inference. Depending on the application, this may be more or less desirable. For example, for generating synthetic training data for a downstream AV model, we may want to have more variability in the generated samples. On the other hand, for driving a 3D avatar using speech, we may care more about the fidelity of the samples at the expense of diversity. Therefore, we provide some sampling strategies to trade-off diversity for fidelity to the speech signal: (1) KNN-based sampling, (2) code averaging, and (3) rejection sampling using a pre-trained synchronization network. For each strategy, as shown in Figure 1c, we sample multiple codes and aggregate their embeddings before passing the result as the next input to the temporal model.

KNN-based sampling. For simplicity of notation, let $e_t := \tilde{e}(\mathbf{j}_t)$ denote the sampled and reconstructed quantized embedding for time t . We replace the sampled code at time step t with the mean of a local Gaussian approximated from its nearest neighbors on the sampling manifold. Let \mathcal{E} denote a set of N codes sampled at time step t . We take the estimate \hat{e}_t to be the mean of the set $\{e \in \mathcal{E} \mid |e - e_t| \leq |\text{KNN}_k(e_t, \mathcal{E}) - e_t|\}$, where $\text{KNN}_k(e_t, \mathcal{E})$ denotes the k -th nearest neighbors of e_t in \mathcal{E} . The replacement code \hat{e}_t is projected to the discrete codebook.

Code averaging. We replace the sampled code e_t with an embedding \hat{e}_t given by the mean of \mathcal{E} , a set of N codes sampled at time step t . The averaged embedding \hat{e}_t is projected to the discrete codebook.

SyncNet-based Sampling. Inspired by classifier-based

rejection sampling in image synthesis, we propose a simple sampling scheme based on a pretrained synchronization network. Specifically, at each time point t , we sample and decode a set of N codes. Each code e_t is decoded by the RVQ autoencoder and scored using a pretrained synchronization network.

While these sampling strategies increase the computational overhead of inference, we can amortize them by distilling the modified sampling distributions into a student network that can be run with no additional cost during inference. We do so by relabeling the code inputs as well as targets of the depth network by the ones obtained from discretizing the aggregated samples (see Supplemental Materials for details).

4. Experiments

4.1. Benchmark Datasets

Most of the existing works on speech-driven 3D facial motion synthesis use VOCASet [9] and BIWI [17] for benchmarking. These datasets are small with a limited number of speakers, and models are often trained and evaluated in a speaker-specific manner on these datasets. Because of their small scale and limited speaker diversity, these datasets do not fully capture the complex relationship between speech and facial motions. While MeshTalk [33] uses a large, multi-speaker dataset to train their model, their dataset is proprietary and not available for public use.

To address this issue, we introduce two large-scale audio-mesh benchmark datasets. These datasets are created by processing videos from the publicly-available VoxCeleb2 video dataset [7] using two monocular face reconstruction methods: DECA [18], a state-of-the-art method for face reconstruction, and SPECTRE [19], a recent method that holds the state-of-the-art for preserving visual speech information. These two datasets contain face meshes at different granularity enabling us to assess how well different speech-driven facial motion synthesis methods fare on different types of meshes. Table 1 shows the statistics of the different datasets. Note that VoxCeleb2 is orders of magnitude larger than the existing benchmark datasets, enabling the development of models that capture speaker diversity reflective of a real-world population.

4.2. Metrics

Lip Vertex Error. In existing works, lip vertex error is used as the main proxy for lip articulation quality. This metric is calculated as

$$\ell_{vertex}(x, \hat{x}) := \max_{t, i \in \text{lip}} \|\mathbf{x}_{ti} - \hat{\mathbf{x}}_{ti}\|_2 \quad (4)$$

where x is the ground truth mesh, \hat{x} is the synthesized mesh, the maximum is taken over all lip vertices and time frames

Dataset	# Mesh Sequences	# Speakers
VOCASet	480	12
BIWI	1109	14
VoxCeleb2 (Mesh)	>1M	6,112

Table 1. **Comparison of Different Benchmark Datasets for Speech-Driven 3D Facial Animation.** Our proposed benchmark datasets of meshes reconstructed from VoxCeleb2 are significantly larger than existing benchmark datasets.

for a given mesh sequence. However, there is a distribution of possible lip vertex positions for a given individual and utterance, and the ground truth is only one sample from this distribution. Lip vertex error does not reflect that a probabilistic model may correctly capture multiple modes that include the ground truth, but receive a large lip vertex error by sampling a different mode. While the lip vertex error measures the precision of the model, or how close every sample is to the ground truth, a more suitable metric for a probabilistic model may be whether any one of several samples, or their mean, is close to the ground truth, which mitigates the impact of diversity on this metric.

Coverage Error. To provide a notion of how close the ground truth is to the sampling distribution of a probabilistic model, we propose to generate a set of samples \mathcal{S} and computing the closest distance to the ground truth:

$$\ell_{cover} := \min_{\hat{x} \in \mathcal{S}} \ell_{vertex}(x, \hat{x}).$$

Intuitively, a probabilistic model with small ℓ_{cover} has a mode that is close to the ground truth, even if a generated sample is not.

Mean Estimate Error. Finally, we also propose to compute the lip vertex error over the mean of \mathcal{S} , i.e., $\ell_{mean} := \ell_{vertex}(x, \mathbb{E}_{\mathcal{S}} \hat{x})$, to assess how close the mean of the sampling distribution is to the ground truth. Both coverage error and the error of the mean error better reflect whether a probabilistic model is capable of generating the ground truth lip sequence better than computing error from one random sample. Note that all three lip errors are the same for deterministic methods, as they are only capable of generating the same sample.

SyncNet Score. While lip vertex errors measure how close generated lip articulations are to the ground truth, they do not reflect whether a particular 3D mesh sequence falls into the possible distribution of facial motions conditioned on a speech utterance. We propose to learn this distribution by training a speech-mesh synchronization network that scores how well a mesh corresponds to a given audio, analogous to the lip synchronization metric used in speech-driven video synthesis [8]. Specifically, we pretrain two different synchronization networks to assess the alignment between

a mesh sequence and an audio signal. In the first network, a multimodal fusion network is used to merge mesh and audio embeddings along the temporal dimension, and a score is computed from the merged embeddings using a linear layer. In the second network, the score is computed directly through the cosine similarity of the normalized mesh and audio embeddings. Both networks are optimized using an InfoNCE contrastive loss [31], and perform well at detecting temporal as well as semantic alignment between audio and 3D face meshes (see Supplemental Materials).

SyncNet Frechet Distance (SyncNet-FD). Beyond measuring the quality of speech synchronization, we also want to measure how well the speech-related facial motions generated by a model capture the realism and diversity of the real distribution of such motions. To do so, we compute the Frechet distance between 1000 SyncNet embeddings of real and generated mesh sequences from our two pretrained speech-mesh synchronization networks.

Style Cosine Similarity and Rank. While the above metrics provide different measures of how well models generate 3D facial motions corresponding to speech, we also want to measure how well models are able to replicate the diverse speaking styles within the datasets. To do so, we train a speaking style recognition model based on ArcFace [11], using 3D facial motions as input (*i.e.*, the deformation of ground truth meshes from the neutral templates). We evaluate how well the models are able to replicate a specific individual’s speaking style by computing the cosine similarity between the embeddings of the reference speaker mesh sequences and the generated mesh sequences. We also compute the rank of the similarity relative to the similarity of all the other speakers in the training set. Details of the implementation and performance of the recognition model are provided in the Supplemental Materials.

Style Frechet Distance (Style-FD). Finally, to assess the diversity of speaking styles produces by the model and how well the distribution matches the speaking styles of the real data, we compute the Frechet Distance between the recognition model embeddings of the real and generated mesh sequences.

4.3. Quantitative Results

Figure 2 shows the results of our comprehensive benchmark. We train recent deterministic and probabilistic methods on our DECA and SPECTRE meshes and evaluate them using our proposed metrics. Overall, our method outperforms the existing methods on realism/diversity (as measured by averaged FD score), speech synchronization, and lip coverage and mean estimate errors. We provide a thorough discussion below.

Ours vs. Deterministic Methods. Existing deterministic

methods¹ suffer in realism/diversity as measured by averaged FD (y-axis, lower is better) on both DECA (Figure 2a) and SPECTRE meshes (Figure 2b). Specifically, VOCA [9] and Faceformer [16] are deterministic methods that directly regress 3D mesh vertices on speech, either using a sliding window (VOCA) or an auto-regressive transformer (FaceFormer). Both methods are susceptible to the over-averaging effect of the regression loss, which is exacerbated by training on large-scale datasets. We observe that FaceFormer produces less stiff motions compared to VOCA, due to conditioning on a longer context provided by auto-regressive modeling, resulting in higher synchronization scores. We add conditioning on a reference speaker sequence to FaceFormer to further reduce the distribution of possible facial motions (FaceFormer+Style). This improves its scores across all metrics, particularly on the SPECTRE meshes that are more detailed, but does not resolve the realism/diversity gap.

Our method also outperforms VOCA and Faceformer on speech synchronization, as measured by the sync score in Figures 2(a-b) (x-axis, higher is better). On the SPECTRE meshes (b), FaceFormer+Style achieves higher SyncNet score compared to default sampling from our probabilistic model, but we can achieve better results using our proposed sampling strategies, as illustrated by the green and blue markers (see later section for discussion). For lip vertex errors, VOCA and FaceFormer both achieve lower ℓ_{vertex} (Figure 2(a-b), marker size, smaller is better), but this is mainly because this metric penalizes the diversity of samples generated by our probabilistic modeling. When we compute the lip vertex error over the average of many samples from our model (Figure 2(c), y-axis, lower is better) ($\ell_{mean}, |\mathcal{S}| = 100$), effectively reducing the effect of sampling diversity, we outperform VOCA and FaceFormer and are able to match the lip vertex error of FaceFormer+Style. Furthermore, our model achieves better coverage error than FaceFormer+Style (Figure 2c, x-axis, lower is better), indicating that our sampling distribution is actually much closer to the ground truth lip vertices.

Ours vs. MeshTalk. MeshTalk [33] is a two-stage method that first learns a discrete Gumbel-Softmax autoencoder [22] that disentangles upper and lower face motion, then trains a probabilistic auto-regressive model over the discrete codes using a convolutional architecture. While the second stage model is probabilistic, disentangling the lower face involves regressing the vertices from audio over sliding windows, similar to VOCA. We observe that MeshTalk is susceptible to the same over-smoothing effects on the lower face, achieving similar synchronization scores to VOCA in Figure 2(a-b). Overall, our method achieves better synchronization as well as realism/diversity compared to MeshTalk and MeshTalk+Style, as reflected in higher sync scores and

¹We defer discussion of CodeTalker [38] to the Supplement.

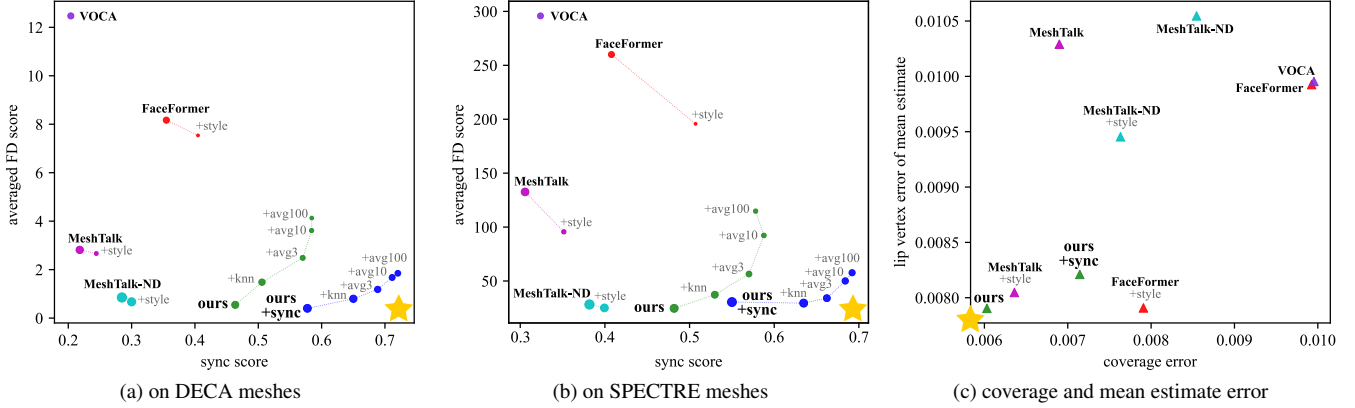


Figure 2. **Benchmark results.** We evaluate all methods on the aggregate SyncNet score and averaged FD score on (a) DECA and (b) SPECTRE meshes from VoxCeleb2. The size of the dots indicates the lip vertex error. Averaged FD score refers to the average between both SyncNet-FD scores. (c) shows the coverage error and the lip vertex error of the mean estimate over 100 samples per speech input on DECA meshes from VoxCeleb2. The yellow star indicates the direction of the best methods. For averaged FD score, lower is better. For sync score, higher is better. For both coverage and mean estimate error, lower is better. See supplementary material for the complete table.

lower averaged FD score. For lip vertex error (ℓ_{vertex}), our meshes are more diverse, and thus deviate from the ground truth meshes more than MeshTalk+Style. However, we achieve better coverage error as well as mean estimate error, suggesting that while our results are more diverse, our sampling distribution is actually closer to the ground truth.

We also train a version of MeshTalk without the regression loss in the codebook (MeshTalk-ND, MeshTalk-ND+Style), for a more direct comparison to another probabilistic auto-regressive model that predicts discrete latent codes. Compared to the original version, MeshTalk-ND and MeshTalk-ND+Style are more diverse, as evidenced by lower SyncNet-FD scores, and they are not susceptible to smoothing of the lower face, as evidenced by improved synchronization scores. However, the quality of the lip articulation suffers. Note that MeshTalk-ND+Style cannot cover the ground truth lip sequences as well as MeshTalk+Style or our approach, even though ours is just as diverse. Our approach also achieves higher synchronization scores. This demonstrates the effectiveness of our probabilistic model design choices in maintaining faithfulness to the driving speech signal.

Trading off Diversity for Fidelity. By design, our probabilistic model learns the entire training distribution of RVQ codes, which is noisy and can result in sampling codes that are less faithful to the conditioning speech during inference. The results in Figure 2(a-b) show that we are able to trade-off diversity for greater fidelity using the strategies in Section 3.3 with (blue) or without (green) SyncNet-based rejection sampling. KNN-based sampling achieves a mild trade-off, as code aggregation is based on a local Gaussian approximation. Code averaging achieves a larger trade-off, as the model samples codes that are closer to

the conditional mean $\mathbb{E}[\mathbf{x}_t | \mathbf{x}_{<t}, \mathbf{y}, \mathbf{s}]$. When averaging between large numbers of codes, eventually the synchronization score decreases due to over-smoothing.

Speaker Style Evaluation. Next, we evaluate the ability of our method to generate the diverse speaking styles of unseen speakers, provided with a reference clip from the target speaker. The results are shown in Table 2, and we compare to other methods that are also trained using a reference clip. Overall, we find that FaceFormer+Style and MeshTalk+Style, which both employ some form of regression from speech in the training stage, are unable to match the speaking style of the target speakers due to over-smoothing and loss of diversity in the facial motions. This is reflected not only in the style cosine similarity, but also in the higher Style-FD. As previous works have noted that recognition networks may be sensitive to slight perturbations introduced by discrete coding schemes [32], we evaluate our method and MeshTalk-ND+Style on the decompressed ground truth meshes of their respective codebook. We find this improves the style matching scores of both models, which approach the scores of the real ground truth meshes.

Key Design Choices for AR Modeling. One challenge of our task is capturing the diverse facial motions corresponding to speech while maintaining faithfulness to speech signal. In Table 3, we show the results of ablation studies that highlight our key design choices. First, using a convolutional architecture for the auto-regressive modeling, as in MeshTalk, results in significantly worse sync scores. Second, incorporating style information early in the temporal AR model, rather than the depth AR model, as done in many works that condition on global embeddings, significantly impairs the synchronization score.

DECA	Style Cosine Similarity \uparrow	Style Rank \downarrow	Style FD \downarrow
FaceFormer+Style	0.127	1596.422	58.652
MeshTalk+Style	0.229	1135.0	38.535
MeshTalk-ND+Style	0.629	53.8	17.068
Ours	0.707	7.3	21.038
GT	0.7644	10.691	-
SPECTRE	Style Cosine Similarity \uparrow	Style Rank \downarrow	Style FD \downarrow
FaceFormer+Style	0.237	650.128	41.062
MeshTalk+Style	0.231	955.3	69.224
MeshTalk-ND+Style	0.609	38.8	20.560
Ours	0.673	20.5	23.533
GT	0.7522	4.982	-

Table 2. **Style Similarity Scores** show that our probabilistic approach can synthesize facial motion closer to the reference style compared to other deterministic methods. See text for details.

Method	Style Cosine Similarity \uparrow	Sync Score \uparrow	Sync FD \downarrow
AR-ConvNet (no style)	-	0.217	9.58
AR-Transformer (no style)	-	0.442	4.21
AR-Transformer+ES	0.315	0.287	2.95
Ours	0.298	0.4634	3.21

Table 3. **Key Ablations** of our model. We show that the design of the auto-regressive model is crucial for proper synchronization.

	Style Matching	Lip Realism	Upper Face Realism
Ours vs. VOCA	85.1/8.5/6.4	70.2/17.0/12.8	80.9/4.3/14.9
Ours vs. FaceFormer	74.4/20.5/5.1	59.0/35.9/5.1	71.1/26.3/2.6
Ours vs. CodeTalker	78.8/9.1/12.1	87.9/3.0/9.1	90.9/3.0/6.1
Ours vs. Faceformer+Style	75.0/11.1/13.9	86.1/8.3/5.6	94.4/2.8/2.8

Table 4. **Results of a Perceptual Study**. Results show percentage of survey respondents who preferred Ours / Baseline / Neither on each of the categories. For style matching, users were provided a reference clip in addition to two videos and asked which one matched the style in the clip better, which one had more realistic lower lip motion, and which one had more realistic upper face motion.

Training Data Type	Training Data Corpus	WER \downarrow
Audio-only	LRS3 trainval+pretrain	18.7
Real AV	LRS3 trainval	30.7
+ Faceformer Synthetic Dataset	LRS3 pretrain	13.4
+ Ours Synthetic Dataset	LRS3 pretrain	7.1
+ Real AV	LRS3 pretrain	8.0

Table 5. **Synthetic Data Generation for AVSR** Training an audio-visual speech recognition model on synthetic meshes generated by our model improves WER over training on meshes extracted from ground truth videos.

4.4. Applications

We showcase two useful applications of a probabilistic model trained on a diverse large-scale dataset. The first application is the ability to generate more natural and realistic 3D facial motions that capture a diversity of real-

world speaking styles, including being able to match the style from a reference clip. We show the results of user ratings in Table 4, illustrating that our approach is strongly preferred over prominent deterministic methods trained on smaller, high-quality datasets, as well as FaceFormer+Style trained on our large-scale datasets. Second, we demonstrate the utility of probabilistic methods for generating synthetic training data for downstream audio-visual tasks. Specifically, we consider the challenging task of noisy audio-visual speech recognition (noisy-AVSR) on the Lip Reading Sentences 3 (LRS3) dataset. High-quality synthetic training data is immensely useful for audio-visual speech recognition, not only because labeled audio-visual corpora are limited, but also because there may be privacy concerns with training and deploying a model on real user data. We show that synthetic data from our speech-driven 3D facial animation model can greatly improve the performance of such audio-visual models, even compared to training on the ground truth visual data. We use our model trained on SPECTRE meshes to generate a large, synthetic 3D facial mesh dataset corresponding to the audio in the “pre-train” subset of the LRS3 dataset and use the detailed lip meshes as input to the downstream model. As shown in Table 5, training an audio-visual speech recognition model on this synthetic visual corpus improves relatively the WER of the model on the test set of LRS3 by 11.3% compared to training on the ground truth lip meshes, and by 47% compared to training on meshes generated by FaceFormer (also trained on SPECTRE meshes). Beyond creative applications, this demonstrates the practical usage of non-deterministic 3D facial mesh synthesis methods for training downstream audio-visual models.

5. Conclusion

In this work, we propose a new large-scale dataset, metrics, and methodology to address the task of probabilistic speech-driven 3D facial motion synthesis. We show the advantages of probabilistic approaches to this task in capturing diversity and propose a careful model design and sampling strategies to ensure strong lip synchrony. We benchmark existing methods on our large-scale dataset, analysing the strengths and weaknesses of each approach. Our probabilistic model outperforms the existing methods across metrics capturing realism, diversity and lip synchronization. Furthermore, we demonstrate new uses of probabilistic models trained on our large-scale dataset for (i) generating 3D facial motion that matches real-world speaking styles through a reference clip, as well as (ii) generating synthetic training data for a downstream audio-visual speech recognition task, which are only possible due to the diversity captured by the dataset and probabilistic model. This work provides a useful large-scale benchmark and analysis tools for other researchers working on this task.

Acknowledgment We thank Zak Aldeneh, Barry Theobald, Masha Fedzechkina Donaldson, Dianna Yee, and Hadi Pour Ansari for helpful discussions and feedback on the paper.

References

- [1] Triantafyllos Afouras, Joon Son Chung, and Andrew Zisserman. Lrs3-ted: a large-scale dataset for visual speech recognition. *arXiv preprint arXiv:1809.00496*, 2018. **2**
- [2] Robert Anderson, Bjorn Stenger, Vincent Wan, and Roberto Cipolla. Expressive visual text-to-speech using active appearance models. In *Proceedings of the IEEE conference on computer vision and pattern recognition*, pages 3382–3389, 2013. **2**
- [3] Alexei Baevski, Yuhao Zhou, Abdelrahman Mohamed, and Michael Auli. wav2vec 2.0: A framework for self-supervised learning of speech representations. *Advances in neural information processing systems*, 33:12449–12460, 2020. **13**
- [4] Yong Cao, Wen C Tien, Petros Faloutsos, and Frédéric Pighin. Expressive speech-driven facial animation. *ACM Transactions on Graphics (TOG)*, 24(4):1283–1302, 2005. **2**
- [5] Lele Chen, Ross K Maddox, Zhiyao Duan, and Chenliang Xu. Hierarchical cross-modal talking face generation with dynamic pixel-wise loss. *arXiv preprint arXiv:1905.03820*, 2019. **2**
- [6] Joon Son Chung, Amir Jamaludin, and Andrew Zisserman. You said that? *arXiv preprint arXiv:1705.02966*, 2017. **2**
- [7] Joon Son Chung, Arsha Nagrani, and Andrew Zisserman. Voxceleb2: Deep speaker recognition. *arXiv preprint arXiv:1806.05622*, 2018. **2, 5, 13, 15**
- [8] Joon Son Chung and Andrew Zisserman. Out of time: automated lip sync in the wild. In *Computer Vision—ACCV 2016 Workshops: ACCV 2016 International Workshops, Taipei, Taiwan, November 20–24, 2016, Revised Selected Papers, Part II 13*, pages 251–263. Springer, 2017. **5**
- [9] Daniel Cudeiro, Timo Bolkart, Cassidy Laidlaw, Anurag Ranjan, and Michael J Black. Capture, learning, and synthesis of 3d speaking styles. In *Proceedings of the IEEE/CVF Conference on Computer Vision and Pattern Recognition*, pages 10101–10111, 2019. **1, 2, 3, 5, 6, 12, 13**
- [10] Radek Daněček, Kiran Chhatre, Shashank Tripathi, Yandong Wen, Michael J Black, and Timo Bolkart. Emotional speech-driven animation with content-emotion disentanglement. *arXiv preprint arXiv:2306.08990*, 2023. **1, 3**
- [11] Jiankang Deng, Jia Guo, Niannan Xue, and Stefanos Zafeiriou. Arcface: Additive angular margin loss for deep face recognition. In *Proceedings of the IEEE/CVF conference on computer vision and pattern recognition*, pages 4690–4699, 2019. **6, 11**
- [12] Zhigang Deng, Pei-Ying Chiang, Pamela Fox, and Ulrich Neumann. Animating blendshape faces by cross-mapping motion capture data. In *Proceedings of the 2006 symposium on Interactive 3D graphics and games*, pages 43–48, 2006. **3**
- [13] Pif Edwards, Chris Landreth, Eugene Fiume, and Karan Singh. Jali: an animator-centric viseme model for expressive lip synchronization. *ACM Transactions on graphics (TOG)*, 35(4):1–11, 2016. **2**
- [14] Tony Ezzat and Tomaso Poggio. Miketalk: A talking facial display based on morphing visemes. In *Proceedings Computer Animation’98 (Cat. No. 98EX169)*, pages 96–102. IEEE, 1998. **2**
- [15] Tony Ezzat and Tomaso Poggio. Visual speech synthesis by morphing visemes. *International Journal of Computer Vision*, 38:45–57, 2000. **2**
- [16] Yingruo Fan, Zhaojiang Lin, Jun Saito, Wenping Wang, and Taku Komura. Faceformer: Speech-driven 3d facial animation with transformers. In *Proceedings of the IEEE/CVF Conference on Computer Vision and Pattern Recognition*, pages 18770–18780, 2022. **1, 2, 3, 6, 12, 13**
- [17] Gabriele Fanelli, Juergen Gall, Harald Romsdorfer, Thibaut Weise, and Luc Van Gool. A 3-d audio-visual corpus of affective communication. *IEEE Transactions on Multimedia*, 12(6):591–598, 2010. **1, 2, 5, 12, 13**
- [18] Yao Feng, Haiwen Feng, Michael J Black, and Timo Bolkart. Learning an animatable detailed 3d face model from in-the-wild images. *ACM Transactions on Graphics (ToG)*, 40(4):1–13, 2021. **2, 5, 15**
- [19] Panagiotis P Filntisis, George Retsinas, Foivos Paraperas-Papantoniou, Athanasios Katsamanis, Anastasios Roussos, and Petros Maragos. Spectre: Visual speech-informed perceptual 3d facial expression reconstruction from videos. In *Proceedings of the IEEE/CVF Conference on Computer Vision and Pattern Recognition*, pages 5744–5754, 2023. **2, 5, 15**
- [20] Jiazhi Guan, Zhanwang Zhang, Hang Zhou, Tianshu Hu, Kaisiyuan Wang, Dongliang He, Haocheng Feng, Jingtuo Liu, Errui Ding, Ziwei Liu, et al. Stylesync: High-fidelity generalized and personalized lip sync in style-based generator. In *Proceedings of the IEEE/CVF Conference on Computer Vision and Pattern Recognition*, pages 1505–1515, 2023. **2**
- [21] Yudong Guo, Keyu Chen, Sen Liang, Yong-Jin Liu, Hujun Bao, and Juyong Zhang. Ad-nerf: Audio driven neural radiance fields for talking head synthesis. In *Proceedings of the IEEE/CVF International Conference on Computer Vision*, pages 5784–5794, 2021. **3**
- [22] Eric Jang, Shixiang Gu, and Ben Poole. Categorical reparameterization with gumbel-softmax. *arXiv preprint arXiv:1611.01144*, 2016. **6**
- [23] Gregor A Kalberer, Pascal Müller, and Luc Van Gool. Speech animation using viseme space. In *VMV*, pages 463–470, 2002. **2**
- [24] Gregor A Kalberer and Luc Van Gool. Face animation based on observed 3d speech dynamics. In *Proceedings Computer Animation 2001. Fourteenth Conference on Computer Animation (Cat. No. 01TH8596)*, pages 20–251. IEEE, 2001. **2**
- [25] Tero Karras, Timo Aila, Samuli Laine, Antti Herva, and Jaakko Lehtinen. Audio-driven facial animation by joint end-to-end learning of pose and emotion. *ACM Transactions on Graphics (TOG)*, 36(4):1–12, 2017. **3**
- [26] Diederik P Kingma and Jimmy Ba. Adam: A method for stochastic optimization. *arXiv preprint arXiv:1412.6980*, 2014. **14**
- [27] Doyup Lee, Chiheon Kim, Saehoon Kim, Minsu Cho, and Wook-Shin Han. Autoregressive image generation using

- residual quantization. In *Proceedings of the IEEE/CVF Conference on Computer Vision and Pattern Recognition*, pages 11523–11532, 2022. [3](#), [4](#), [14](#)
- [28] DW Massaro, MM Cohen, M Tabain, J Beskow, and R Clark. Animated speech: research progress and applications. 2012. [2](#)
- [29] Gaurav Mittal and Baoyuan Wang. Animating face using disentangled audio representations. In *Proceedings of the IEEE/CVF Winter Conference on Applications of Computer Vision*, pages 3290–3298, 2020. [2](#)
- [30] Evonne Ng, Hanbyul Joo, Liwen Hu, Hao Li, Trevor Darrell, Angjoo Kanazawa, and Shiry Ginosar. Learning to listen: Modeling non-deterministic dyadic facial motion. In *Proceedings of the IEEE/CVF Conference on Computer Vision and Pattern Recognition*, pages 20395–20405, 2022. [3](#)
- [31] Aaron van den Oord, Yazhe Li, and Oriol Vinyals. Representation learning with contrastive predictive coding. *arXiv preprint arXiv:1807.03748*, 2018. [6](#), [11](#)
- [32] Ali Razavi, Aaron Van den Oord, and Oriol Vinyals. Generating diverse high-fidelity images with vq-vae-2. *Advances in neural information processing systems*, 32, 2019. [2](#), [7](#)
- [33] Alexander Richard, Michael Zollhöfer, Yandong Wen, Fernando De la Torre, and Yaser Sheikh. Meshtalk: 3d face animation from speech using cross-modality disentanglement. In *Proceedings of the IEEE/CVF International Conference on Computer Vision*, pages 1173–1182, 2021. [1](#), [2](#), [3](#), [5](#), [6](#), [14](#)
- [34] Sarah Taylor, Taehwan Kim, Yisong Yue, Moshe Mahler, James Krahe, Anastasio Garcia Rodriguez, Jessica Hodgins, and Iain Matthews. A deep learning approach for generalized speech animation. *ACM Transactions On Graphics (TOG)*, 36(4):1–11, 2017. [2](#)
- [35] Sarah L Taylor, Moshe Mahler, Barry-John Theobald, and Iain Matthews. Dynamic units of visual speech. In *Proceedings of the 11th ACM SIGGRAPH/Eurographics conference on Computer Animation*, pages 275–284, 2012. [2](#)
- [36] Aaron Van Den Oord, Oriol Vinyals, et al. Neural discrete representation learning. *Advances in neural information processing systems*, 30, 2017. [3](#)
- [37] Ashish Verma, Nitendra Rajput, and L Venkata Subramaniam. Using viseme based acoustic models for speech driven lip synthesis. In *2003 IEEE International Conference on Acoustics, Speech, and Signal Processing, 2003. Proceedings. (ICASSP'03).*, volume 5, pages V–720. IEEE, 2003. [2](#)
- [38] Jinbo Xing, Menghan Xia, Yuechen Zhang, Xiaodong Cun, Jue Wang, and Tien-Tsin Wong. Codetalker: Speech-driven 3d facial animation with discrete motion prior. In *Proceedings of the IEEE/CVF Conference on Computer Vision and Pattern Recognition*, pages 12780–12790, 2023. [1](#), [2](#), [3](#), [6](#), [11](#), [12](#), [13](#)
- [39] Yuyu Xu, Andrew W Feng, Stacy Marsella, and Ari Shapiro. A practical and configurable lip sync method for games. In *Proceedings of Motion on Games*, pages 131–140. 2013. [2](#)
- [40] Chenxu Zhang, Yifan Zhao, Yifei Huang, Ming Zeng, Saifeng Ni, Madhukar Budagavi, and Xiaohu Guo. Facial: Synthesizing dynamic talking face with implicit attribute learning. In *Proceedings of the IEEE/CVF international conference on computer vision*, pages 3867–3876, 2021. [2](#)
- [41] Yang Zhou, Zhan Xu, Chris Landreth, Evangelos Kalogerakis, Subhansu Maji, and Karan Singh. Visemenet: Audio-driven animator-centric speech animation. *ACM Transactions on Graphics (TOG)*, 37(4):1–10, 2018. [2](#)

Supplementary Materials

Probabilistic Speech-Driven 3D Facial Motion Synthesis: New Benchmarks, Methods, and Applications

A. Supplemental Video

Please see the **accompanying video** for an overview of our work and qualitative examples from our model.

B. Overview

The following sections provide additional methodology and/or results that were not included in the main paper.

Section C provides more details on the metrics, including (i) limitations of maximal lip vertex error for evaluating probabilistic models and (ii) details of the pretrained models used for evaluation.

Section D provides the complete table of benchmark results corresponding to Figure 2 of the main paper, a discussion of CodeTalker [38], and additional ablation results for our model.

Section E discusses *efficiency* of our method, including (i) a knowledge distillation strategy for amortizing the sampling strategies, and (ii) diversity *vs.* efficiency trade-off that can be achieved by sampling fewer codes from our autoregressive model at inference time.

Section F provides implementation and training details that were deferred from the main text.

Section G discusses the limitations and ethical considerations of this work.

C. Metrics

C.1. Limitation of Maximal Lip Vertex Error

Maximal lip vertex error (ℓ_{vertex}) is a metric that measures the maximum difference in lip vertices between the ground truth mesh and a mesh generated from the model. This metric is used as a proxy for lip articulation quality in existing works, but as a standalone metric, it has limitations for evaluating probabilistic models. As shown in Supplemental Figure 3, a probabilistic model (row 2) can generate lip articulation that is more similar to the ground truth (row 1), but due to variations between samples, have larger ℓ_{vertex} compared to a deterministic model (row 3) that generates an over-averaged result. Our proposed lip vertex metrics, ℓ_{cover} and ℓ_{mean} , address this limitation and provide a more complete picture of performance. Overall, there is a need to look across multiple metrics (sync score, FD score, lip vertex error) when evaluating speech-driven 3D facial motion synthesis.

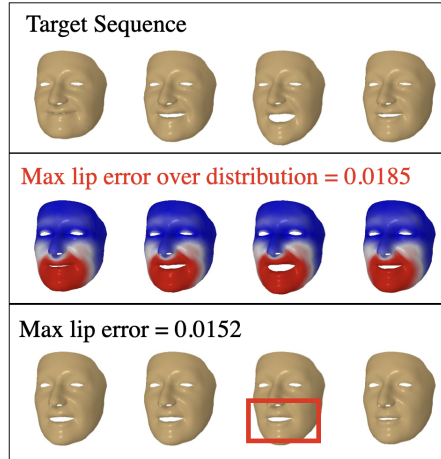


Figure 3. **Limitations of ℓ_{vertex} as a metric.** Probabilistic models (row 2) generate 3D facial motions with diversity, as shown by the color map of standard deviation. They may achieve worse ℓ_{vertex} compared to deterministic models (row 3), despite being able to generate a mesh sequence that matches the ground truth sequence better (row 1). See text for details.

C.2. Audio-Mesh Synchronization Networks

The audio-mesh synchronization networks are trained using InfoNCE contrastive loss [31] with a batch size of 64, *i.e.*, for each 3D mesh sequence, we sample 63 negative audio examples that are either semantically misaligned (taken from a different clip) or temporally misaligned (taken from a different time point of the same clip). Supplemental Figure 4 shows plots of the models evaluated on held-out ground truth audio-mesh pairs with increasing temporal misalignment. The results indicate that all the pretrained networks are sensitive to individual frames of audio-mesh misalignment.

C.3. Speaking Style Recognition Network

The style recognizer is trained on 3D facial motion (deformation between animated and neutral face meshes). The facial motion encoder uses a similar architecture as our RVQ encoder with standard 1D convolutional blocks instead of causal 1D convolutional blocks. We use angular margin loss [11] to maximize the cosine similarity between embeddings from the same speaker while minimizing cosine similarity with other speakers. The performance of the models for DECA and SPECTRE are shown in the GT line

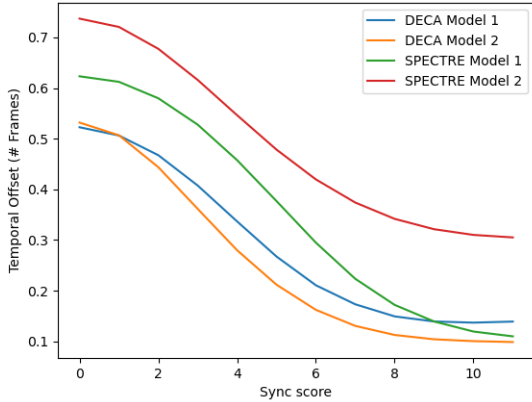


Figure 4. **SyncNet Evaluation** All of our synchronization networks can detect individual frames of temporal shift between audio and 3D facial mesh sequences.

of Table 2 in the main paper.

D. Additional Results

D.1. Complete Table - Main Figure 2

Supplemental Table 6 shows the full results corresponding to Figure 2 of the main paper. Our approach outperforms the existing methods across the board. Importantly, while deterministic methods (*i.e.*, Faceformer+Style) achieve good lip synchronization and lip vertex error, they suffer in diversity/realism as highlighted in **red**.

Sync score Existing deterministic methods (FaceFormer, Faceformer+Style) achieve better synchronization than existing probabilistic methods (Meshtalk, MeshTalk-ND, MeshTalk+Style, MeshTalk-ND+Style). Our probabilistic method achieves the highest sync scores out of all methods, particularly when we use our sampling strategies to trade off diversity for greater speech fidelity (Ours+Avg100).

Frechet distance Deterministic methods (VOCA, Faceformer, Faceformer+Style) suffer on this metric, as highlighted in **red**, suggesting that the generated facial motions are unrealistic. The probabilistic methods perform better on this metric, with our method outperforming MeshTalk on three out of four cases.

Maximal Lip Vertex Error Deterministic methods (VOCA, Faceformer, Faceformer+Style) achieve lower ℓ_{vertex} , which measures the maximum vertex error between the ground truth and one synthesized mesh sequence. However, this does not take into account the diversity of probabilistic methods. When we compute the maximal vertex error between the ground truth and the average of many synthesized sequences (ℓ_{mean}), our approach matches Faceformer+Style and outperforms the others. We

also achieve the lowest coverage error (ℓ_{cover}), suggesting that the ground truth sequences are closest to our sampling distribution. Finally, when we use sampling strategies (Ours+Avg100), we are able to trade off the coverage of our model (ℓ_{cover}) for improved precision (ℓ_{vertex}).

D.2. Discussion of CodeTalker

CodeTalker [38] extends Faceformer [16] using a vector-quantized (VQ) autoencoder to learn a discrete 3D facial motion prior. While Faceformer uses an auto-regressive transformer to directly regress 3D mesh deformations, CodeTalker uses an auto-regressive transformer to regress the embeddings of the ground truth meshes in the latent space. Their training loss consists of a combination of regression errors over the embeddings and the original 3D mesh deformations after decoding, and training occurs in a teacher-forcing manner. During inference, the predicted embeddings are projected to the nearest codes in the VQ codebook before being decoded to produce 3D facial motion. The motivation is that the projection to the VQ codebook selects a mode in the distribution of 3D facial motions, whereas Faceformer regresses to the conditional mean of motion and produces over-smoothed outputs that do not correspond to any mode. Importantly, while their auto-regressive model selects codes from a pretrained codebook, it is deterministic and selects a code that is nearest to the regressed latent embedding.

We trained the original implementation of CodeTalker by the authors on our data, as well as our own re-implementation using our RVQ codebook and auto-regressive architecture. While training the VQ codebook produced good reconstructions of 3D facial motion, we found that training the auto-regressive model using the combination of regression losses failed to converge to a reasonable result on our data. This is likely due to the large scale and diversity of our dataset compared to VocaSet [9] and BIWI [17], which leads to a high-variance, multi-modal distribution in the latent space that is difficult to regress.

While we are unable to converge to a reasonable result with their original loss, we note that conceptually, taking the *expectation* of the code embeddings sampled from our model at each time point would produce an equivalent result to performing regression in the latent space. In other words, the expected output of CodeTalker can be achieved by performing code averaging as in Section 3.3 with an infinite number of codes. Therefore, we expect the performance of CodeTalker to be the limiting case of the trend of the green points in Figure 2(a-b) of the main text.

D.3. Additional Ablations

Choice of Temporal Model We show preliminary results of our model trained with different temporal models in Supplemental Table 7. We found that using a transformer as

Model	Sync score \uparrow		Fréchet distance \downarrow		Maximal Lip Vertex Error ($\times 10^{-3}$) \downarrow		
DECA	Model 1	Model 2	Model 1	Model 2 \downarrow	ℓ_{vertex}	ℓ_{cover}	ℓ_{mean}
VOCA	0.137	0.271	22.0	2.94	10.0	10.0	10.0
FaceFormer	0.348	0.361	13.9	2.44	9.9	9.9	9.9
MeshTalk	0.262	0.174	5.2	0.48	11.1	6.9	10.3
MeshTalk-ND	0.286	0.284	1.3	0.40	13.2	8.6	10.5
FaceFormer+Style	0.369	0.441	13.2	1.89	7.9	7.9	7.9
MeshTalk+Style	0.286	0.203	4.7	0.64	8.4	<u>6.3</u>	<u>8.1</u>
MeshTalk-ND+Style	0.298	0.302	<u>1.0</u>	<u>0.34</u>	11.9	7.6	9.5
Ours	<u>0.463</u>	<u>0.464</u>	0.9	0.23	10.8	6.0	7.9
Ours+Avg100	0.684	0.600	7.1	1.18	<u>8.3</u>	7.1	8.2
SPECTRE	Model 1	Model 2	Model 1	Model 2 \downarrow	ℓ_{vertex}	ℓ_{cover}	ℓ_{mean}
VOCA	0.357	0.290	524.9	66.8	15.5	15.5	15.5
FaceFormer	0.393	0.423	449.5	70.4	15.6	15.6	15.6
MeshTalk	0.309	0.302	227.9	37.3	17.7	12.4	16.1
MeshTalk-ND	0.327	0.436	49.1	<u>7.4</u>	20.3	13.1	16.0
FaceFormer+Style	0.438	<u>0.576</u>	351.0	40.5	12.8	12.8	12.8
MeshTalk+Style	0.331	0.372	178.5	12.7	<u>13.9</u>	<u>10.2</u>	13.2
MeshTalk-ND+Style	0.325	0.474	<u>43.2</u>	6.9	17.9	11.8	14.5
Ours	<u>0.444</u>	0.520	40.9	8.4	18.2	10.0	<u>13.0</u>
Ours+Avg100	0.565	0.591	199.3	30.3	<u>13.9</u>	11.9	13.7

Table 6. **Benchmark Results** corresponding to Figure 2 in the main paper. Best results in each column are **bolded**, while second best results are underlined. ℓ_{vertex} , ℓ_{cover} , and ℓ_{mean} denote the maximal lip vertex error, coverage error, and mean estimate error respectively and are computed with $|S| = 100$. See Section 4.2 of the main text for descriptions of the metrics.

Temporal Model	Uses Ref. Style?	Sync Score \uparrow	Averaged FD \downarrow
Transformer block	no	0.45	0.51
Ours	no	0.43	0.73
Transformer block	yes	0.43	0.36
Ours	yes	0.44	0.54

Table 7. **Choice of Temporal Model** Comparison of transformer vs. masked convolution blocks for the temporal model on the DECA meshes. See text for details.

Audio Encoder	First Code CE \downarrow	Average Code CE \downarrow
Wav2Vec 2.0 [3]	2.09	2.54
Ours (trained from scratch)	1.97	2.50

Table 8. **Choice of Audio Encoder** Comparison of Wav2Vec 2.0 [3] and our audio encoder trained on scratch on the DECA meshes. CE: cross-entropy loss on held-out set (lower is better). See text for details.

the temporal model in the absence of a reference style clip improves both the synchronization and realism/diversity of the outputs, as measured by sync score and Fréchet distance respectively. However, the results were more varied when

we provide additional information through a reference style clip. Use of a transformer for the temporal model may improve diversity at the cost of synchronization.

Choice of Audio Encoder Several recent works, namely Faceformer [16] and CodeTalker [38] use a self-supervised and pretrained wav2vec 2.0 speech model [3] as the audio encoder. While this may prevent overfitting of the audio encoder on small datasets as VocaSet [9] and BIWI [17], we found that using a pretrained audio encoder was not necessary for a large-scale dataset like VoxCeleb2 [7]. As shown in Supplemental Table 8, in our preliminary experiences, we found that using the pretrained speech model did not improve results.

E. Improving Efficiency

While the focus of the methodology and results in the main paper was primarily on the quality and diversity of the model, for certain applications (e.g., real-time speech-driven 3D avatars), the efficiency of the method is also important. In this section, we elaborate on improving the speed/efficiency of our method.

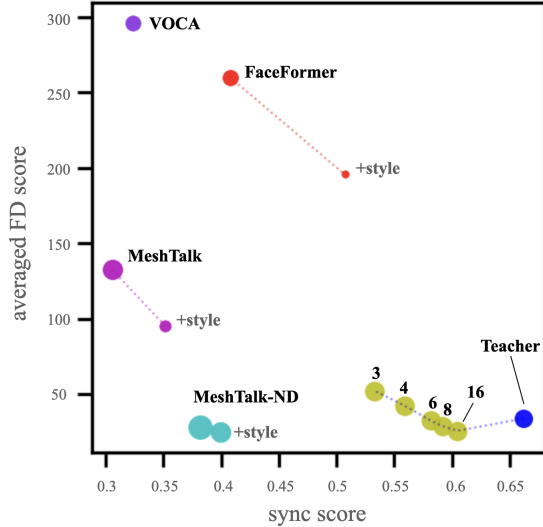


Figure 5. **Improving Model Efficiency** Results are shown for the SPECTRE meshes. See text for details.

E.1. Knowledge Distillation

In Section 3.3 of the main text, we described sampling strategies for trading off the diversity of the auto-regressive model for improved precision and fidelity. However, this strategy increases the inference speed, as multiple codes need to be sampled and aggregated. We propose a knowledge distillation strategy for amortizing this added sampling time. Recall that \mathbf{j} denotes a matrix of codebook indices indexed by time t and depth d corresponding to the real facial motion \mathbf{x} . We obtain the new targets $\hat{\mathbf{j}}$ for the student by:

1. Computing the audio-visual context using the temporal model $\mathbf{h}_{av}[t]$ in a teacher-forcing manner, *i.e.*, inputting the ground truth \mathbf{j} into Equation (2) in the main text.
2. Sampling codes from the depth model using Equation (3) without teacher-forcing. Namely, we use $\mathbf{h}_{av}[t]$ from Step 1 to compute v_{t2} , but use the sampled codes in place of the ground truth codes for computing v_{td} , $d \geq 3$.
3. Aggregating the sampled codes using strategies discussed in Section 3.3 of the main text and reprojecting them to the RVQ codebook to obtain new indices $\hat{\mathbf{j}}$.

The student model is trained in a teacher-forcing manner using both the ground truth codes \mathbf{j} as well as the new targets $\hat{\mathbf{j}}$. Specifically, we use \mathbf{j} as input to the temporal model, and we use $\hat{\mathbf{j}}$ as input to the depth model. We also use $\hat{\mathbf{j}}$ as the targets for optimizing the student model. As shown in Supplemental Figure 5, this enables us to distill the sampled and aggregated labels from a teacher model (blue) to a student model (yellow, ‘16’) with improved inference time.

E.2. Quality vs. Efficiency Trade-off

One of the advantages of the coarse-to-fine design of the RVQ codebook is the possibility of improving efficiency by predicting and decoding codes. We show that this can be done while still achieving high synchronization for as few as 3 codes (out of depth of 16). As shown by the yellow points in Supplemental Figure 5, reducing the number of codes yields a **quality vs. efficiency trade-off**, where we can achieve improved speed/efficiency at the cost of losing finer 3D motions.

F. Implementation Details

RVQ Autoencoder The 3D facial motion encoder and decoder consist of 1D convolutional blocks. The inputs and outputs are 3D facial motion represented by mesh vertex deformations, *i.e.*, the difference between the mesh vertex positions for animated and neutral expressions. The encoder consists of a 1D convolutional layer with kernel size of 1 to aggregate information over mesh vertex deformations, then two 1D causal convolutional layers with kernel size of 3 to aggregate information over time. The decoder consists of the same blocks in the reverse order. For input size $\mathbf{x} \in \mathbb{R}^{T \times 3V}$, the size of the latent embeddings is $Z \in \mathbb{R}^{T \times N_C}$, where N_C is the dimensionality of the codes in codebook \mathcal{C} . In practice, we use a shared codebook [27] with $D = 16$, $|\mathcal{C}| = 256$ and $N_C = 128$.

Audio encoder Following [33], our audio encoder consists of 1D convolutional blocks operating over mel-spectrograms of 1s audio samples centered at each visual frame.

Reference Clip Encoder The reference clip is encoded using the same architecture as the RVQ encoder, except standard convolutional layers are used in place of the causal convolutions.

Two-Stage Auto-Regressive Model The temporal auto-regressive model consists of four masked causal convolutional layers [33] with kernel size of 2 and increasing dilation of 1, 2, 4, 8 for gathering audio-visual context. The depth auto-regressive model consists of a masked transformer self-attention block with embedding size of 64.

Sampling Strategies For KNN-based sampling, we use $N = 100$ and $K = 3$. For SyncNet-based sampling, we take the top 1/2 codes based on the synchronization score. For code averaging, we vary the number of codes averaged depending on the desired diversity vs. fidelity trade-off.

Training We train the RVQ autoencoder and two-stage auto-regressive model for approximately 150 and 200 epochs respectively with Adam optimizer [26] with learning rate of 10^{-4} . For knowledge distillation, we train the student for approximately 100 epochs. The two-stage auto-regressive model is trained in a teacher-forcing manner. We use both stochastic sampling and soft code targets [27].

G. Additional Discussion

Limitations. (1) Our benchmark dataset relies on state-of-the-art monocular face reconstruction techniques [18, 19] and the VoxCeleb2 video dataset [7]. The quality of the face meshes is limited compared to those reconstructed from high-resolution multi-view videos. (2) While our model can achieve real-time synthesis on high-end GPUs, it does not run in real-time on standard consumer-grade hardware. We leave improvements along these directions to future work.

Ethical Considerations. The datasets and models used in this work are intended for research purposes only. While meshes from this work can be used to render photo-realistic content, they should not be used to generate videos of individuals without their consent.